J. Fluid Mech. (2007), *vol.* 578, *pp.* 67–84.
doi:10.1017/S0022112007004983 Printed in the United Kingdom

The initial development of a jet caused by fluid, body and free-surface interaction. Part 2. An impulsively moved plate

D. J. NEEDHAM[1], J. BILLINGHAM[2] AND A. C. KING[1]†

[1]School of Mathematics, University of Birmingham, Birmingham, B15 2TT, UK

[2]School of Mathematical Sciences, University of Nottingham, Nottingham, NG7 2RD, UK

(Received 8 September 2006 and in revised form 27 November 2006)

The free-surface deformation and flow field caused by the impulsive horizontal motion of a rigid vertical plate into a horizontal strip of inviscid incompressible fluid, initially at rest, is studied in the small time limit using the method of matched asymptotic expansions. It is found that three different asymptotic regions are necessary to describe the flow. There is a main, $O(1)$ sized, outer region in which the flow is singular at the point where the free surface meets the plate. This leads to an inner region, centred on the point where the free surface initially meets the plate, with size of $O(-t\log t)$. To resolve the singularities that arise in this inner region, it is necessary to analyse further the flow in an inner-inner region, with size of $O(t)$, again centred upon the wetting point of the nascent rising jet. The solutions of the boundary value problems in the two largest regions are obtained analytically. The solution of the parameter-free nonlinear boundary value problem that arises in the inner-inner region is obtained numerically.

1. Introduction

In King & Needham (1994), the topic of jet development caused by the interaction of moving boundaries and fluids with a free surface was reviewed and further developed. It was noted that this type of flow is rather different from the wedge-entry problems studied by Cointe & Armand (1987), Cointe (1989), Greenhow & Lin (1983), and Howison, Ockendon & Wilson (1991), as it is not self-similar. The solution for a vertical plate accelerated into a stationary horizontal strip of inviscid incompressible fluid was derived and critically compared with previous studies of this problem. This analysis was performed in the small time limit. All the boundary value problems that arise were solved analytically, and expressions for the height that the fluid rises up the plate and the free-surface gradient at the plate were given. In an age when sophisticated computer codes can attempt to solve this problem, the utility of these results is in both providing a test of the accuracy of these codes and giving insights into the structure of the initially evolving flow field. In the case of an accelerating plate, the flow near the point where the free surface meets the plate is dominated by a region of dimension $O(-t^2\log t)$, in which the main feature is the uniform vertical translation of a block of fluid to form the root of any subsequent jet. Corrections to this main primary flow feature determine that the gradient of the free surface where

† Professor King died in January 2005.

it meets the plate is $O(1/\log t)$. Some support for these conclusions can be found in the experimental study of Yong & Chwang (1992).

In this paper we extend our previous work to the case of a plate that moves into an initially stationary strip of fluid with constant velocity $U > 0$. Since the plate is moving with constant velocity when $t > 0$, Galilean invariance allows the results to be interpreted in terms of the problem associated with a slab of fluid impacting upon a stationary plate, with the slab of fluid having velocity U when $t = 0$. In our presentation, however, we will address the problem in terms of the plate impulsively advancing into the initially static slab of fluid when $t = 0$. This flow is rather more violent than in the case of an accelerating plate, and consequently more difficult to analyse. We find that the impulsive boundary motion produces an immediate pressure impulse in the fluid, in contrast to the uniformly accelerating situation. This is singular at the point where the free surface meets the plate at $t = 0^+$. To resolve this singularity it is necessary to consider regions of size $O(-t \log t)$ and then $O(t)$ about this point in order to find a boundary value problem that captures the dynamics of the free surface close to the plate, and is spatially non-singular when $t > 0$ at the point where the free surface meets the plate. The final boundary value problem is nonlinear and parameter-free. As such, it can be calculated with a single computation, which is carried out using the boundary integral method, to find the flow field and free surface near the tip of the nascent jet. Results of this computation are presented and some limitations and applications of this type of analysis are discussed.

The problem of the initial impulsive motion of a plate, treated in this paper, has distinct structural differences, both mathematical and physical, from that of the initial uniformly accelerating motion of the plate, as described in King & Needham (1994), detailed above. This is our primary motivation for studying this classical problem. For initial plate motions with velocity of $O(t^\alpha)$ as $t \to 0^+$, with $\alpha > 0$, which are not impulsive, we expect the main structure to be more closely aligned with that of the uniformly accelerating plate solution, $\alpha = 1$, rather than that of the impulsive plate solution, $\alpha = 0$, studied here. The details in these cases have yet to be worked out, but this is not the purpose of the present investigation. We remark, as in King & Needham (1994), that a possible application of the present analysis is to the situation arising close to the bow of a ship of narrow angle, moving at constant speed into an otherwise stationary fluid; in particular, to the structure of the flow close to the line where the free surface meets the bow of the ship.

2. Equations of motion

We analyse the equations of motion appropriate to the situation when a rigid vertical plate is moved impulsively with constant velocity U into a strip of inviscid incompressible fluid of uniform depth h, that is initially at rest. Since we are interested in the violent flow induced by the impulsive motion of the plate, we will neglect the effects of surface tension but include the gravitational restoring force. Initially the system is at rest, as illustrated in figure 1, where the Cartesian coordinates (x, y) have an origin that is fixed in space for all $t \geqslant 0$, and lies at the point where the plate meets the undisturbed free surface at time $t = 0$.

When $t > 0$ the plate moves into the fluid with constant velocity, and hence lies at $x = Ut$, and drives a free-surface disturbance, $y = \eta(x, t)$. This is shown in figure 2. We will consider this system in the small time limit and therefore express the dependent variables as asymptotic expansions in the small parameter t. Since the

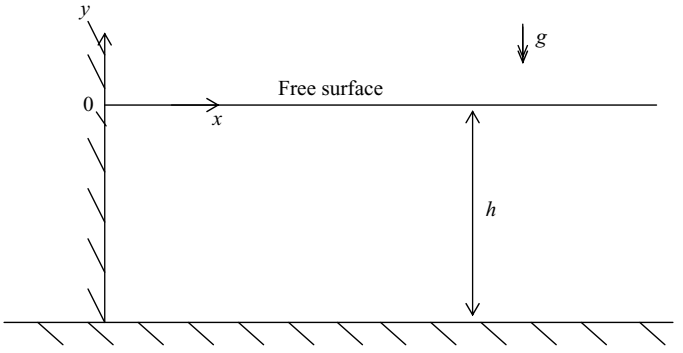

FIGURE 1. Configuration at rest, $t = 0$.

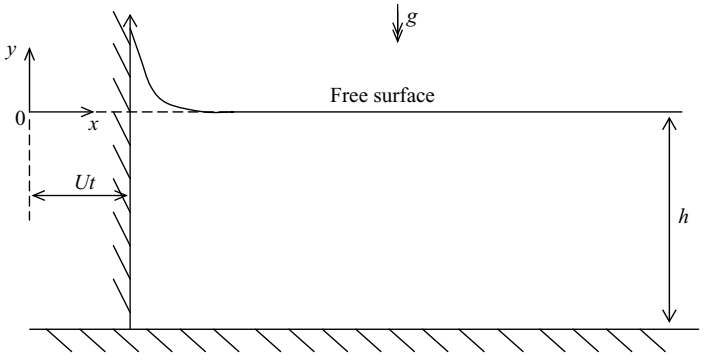

FIGURE 2. Configuration for $t > 0$.

flow is irrotational, it is convenient to work with a velocity potential ϕ, which leads to the usual kinematic and Bernoulli equations on the free surface.

We non-dimensionalize the equations using

$$\bar{x} = \frac{x}{h}, \qquad \bar{y} = \frac{y}{h}, \qquad \bar{\phi} = \frac{\phi}{Uh}, \qquad \bar{\eta} = \frac{\eta}{h}, \qquad \bar{t} = \frac{tU}{h}, \tag{2.1}$$

after which, with the bars dropped for convenience, the mass conservation equation in the fluid is Laplace's equation

$$\phi_{xx} + \phi_{yy} = 0. \tag{2.2}$$

On the plate, which is moving with unit speed, we have

$$\phi_x(t, y, t) = 1. \tag{2.3}$$

The no-flux condition normal to the bed takes the form

$$\phi_y(x, -1, t) = 0, \tag{2.4}$$

and the free-surface conditions applied on $y = \eta(x, t)$ are

$$\phi_y = \eta_t + \phi_x \eta_x \quad \text{(kinematic)}, \tag{2.5}$$

$$\phi_t + \frac{1}{2}\left(\phi_x^2 + \phi_y^2\right) + \frac{\eta}{F^2} = 0 \quad \text{(Bernoulli)}. \tag{2.6}$$

Here $F = U/\sqrt{gh}$, is the Froude number. The far-field conditions are

$$|\nabla\phi|,\ \eta \to 0 \quad \text{as} \quad x \to \infty. \tag{2.7}$$

3. Asymptotic structure as $t \to 0^+$

3.1. *Outer region*

The change in velocity of the plate from zero to unity over an infinitesimal time interval causes a pressure impulse in the fluid (see, for example, Batchelor 1967, p. 471). Once this impulse is created, the flow and free-surface deformation begin when $t = 0^+$. To determine this impulse, we let $t \to 0^+$ in the equations of motion and boundary conditions (where there are time derivatives in an equation we integrate from $t = 0^-$ to $t = 0^+$ and use this to establish conditions at $t = 0^+$). We define $\Pi(x, y) = \phi(x, y, 0^+)$, after which it is straightforward to show that

$$\nabla^2\Pi = 0 \quad \text{in} \quad -1 < y < 0, \quad x > 0, \tag{3.1}$$

$$\Pi_x(0, y) = 1 \quad \text{for} -1 \leqslant y \leqslant 0, \tag{3.2}$$

$$\Pi_y(x, -1) = 0 \quad \text{for } x > 0, \tag{3.3}$$

$$\Pi(x, 0) = 0 \quad \text{for } x > 0, \tag{3.4}$$

$$|\nabla\Pi(x, y)| \to 0 \quad \text{as} \quad x \to \infty, \quad -1 \leqslant y \leqslant 0. \tag{3.5}$$

This problem was solved exactly by D. H. Peregrine (1972, unpublished notes) and further investigated by King & Needham (1994). Introducing standard polar coordinates (r, θ) with respect to the Cartesian coordinates (x, y), the form of $\Pi(r, \theta)$ as $r \to 0$, is given by

$$\Pi(r, \theta) = -\frac{2}{\pi} r \sin\theta \log r + \frac{2}{\pi}\left(1 + \log\frac{4}{\pi}\right) r \sin\theta - \frac{2}{\pi} r\theta \cos\theta + o(r) \tag{3.6}$$

as $r \to 0$ with $\pi/2 \leqslant \theta \leqslant 0$. For $t > 0$ we now expand the velocity potential and free-surface elevation as $\phi = \Pi + t\phi_1 + \ldots$ and $\eta = t\eta_1 + t^2\eta_2 + \ldots$ with $x, y = O(1)$ as $t \to 0^+$. The correction to the impulse potential, ϕ_1, and the leading-order free-surface elevation, η_1, and its correction, η_2, satisfy

$$\nabla^2\phi_1 = 0 \quad \text{in} \quad -1 < y < 0,\ x > 0, \tag{3.7}$$

$$\phi_{1,x} = -\Pi_{xx} \quad \text{on } x = 0,\ -1 \leqslant y \leqslant 0, \tag{3.8}$$

$$\phi_{1,\,y} = 0 \quad \text{on } y = -1,\ x > 0, \tag{3.9}$$

$$\phi_1 = -\tfrac{1}{2}\left(\Pi_x^2 + \Pi_y^2\right) \quad \text{on } y = 0,\ x > 0, \tag{3.10}$$

$$\eta_1 = \Pi_y(x, 0) \quad \text{for } x > 0, \tag{3.11}$$

$$2\eta_2 = \eta_1\Pi_{yy}(x, 0) + \phi_{1y}(x, 0) - \Pi_x(x, 0)\eta_{1x}(x, 0) \quad \text{for } x > 0, \tag{3.12}$$

$$|\nabla\phi_1| \to 0 \quad \text{as} \quad x \to \infty,\ -1 \leqslant y \leqslant 0, \tag{3.13}$$

$$\eta_1, \eta_2 \to 0 \quad \text{as} \quad x \to \infty. \tag{3.14}$$

From (3.11), following King & Needham (1994), we immediately find that

$$\eta_1 \sim \frac{2}{\pi}\log\left(\frac{4}{\pi x}\right) \quad \text{as} \quad x \to 0. \tag{3.15}$$

Since we are principally interested in the solutions near the corner point, $x = y = 0$, we will investigate (3.7)–(3.10) locally at the corner. In the polar coordinate system

introduced above, we need to consider the boundary value problem

$$\nabla^2\phi_1 = 0, \quad -\frac{\pi}{2} < \theta < 0, \quad 0 < r \ll 1, \tag{3.16}$$

$$\frac{\partial\phi_1}{\partial\theta} = \frac{2}{\pi} \quad \text{on} \quad \theta = -\frac{\pi}{2}, \quad 0 < r \ll 1, \tag{3.17}$$

$$\phi_1 = -\frac{2}{\pi^2}\left(\log\frac{4}{\pi} - \log r\right)^2 \quad \text{on} \quad \theta = 0, \quad 0 < r \ll 1, \tag{3.18}$$

where conditions (3.17) and (3.18) are obtained using (3.6), (3.8) and (3.10). We now solve the boundary value problem (3.16)–(3.18) in terms of the expansion

$$\phi_1 = A_1(\theta)\log^2 r + A_2(\theta)\log r + A_3(\theta) + A_4(\theta) r\log^2 r + A_5(\theta) r\log r + A_6(\theta) r + o(r^2\log^2 r)$$

as $r \to 0$, $-\pi/2 \leqslant \theta \leqslant 0$. From this we obtain a sequence of boundary value problems, which are readily soluble to give

$$A_1 = -\frac{2}{\pi^2}, \quad A_2 = \frac{4}{\pi^2}\log\frac{4}{\pi}, \quad A_3 = \frac{2\theta^2}{\pi^2} + \frac{4\theta}{\pi} - \frac{2}{\pi^2}\log^2\frac{4}{\pi},$$
$$A_4 = 0, \quad A_5 = 0, \quad A_6 = k\sin\theta. \tag{3.19}$$

The term $A_6 = k\sin\theta$ represents a non-singular eigensolution to this problem, and the indeterminacy of k arises from the fact that the analysis is local to $r = 0$. However, this is not important here, because the singular terms in the equation are fully determined. On using (3.6), (3.12) and (3.15) and (3.19) we can determine that $\eta_2 \sim 2/(\pi x) + k/2$ as $x \to 0$. To summarize, close to the spatial origin, the expansions in this outer region take the form

$$\begin{aligned}\phi(r,\theta,t) = {} & \left[-\frac{2}{\pi} r\sin\theta\log r + \frac{2}{\pi}\left(1 + \log\frac{4}{\pi}\right) r\sin\theta - \frac{2\theta}{\pi} r\cos\theta + O(r^3)\right] \\ & + t\left[-\frac{2}{\pi^2}\log^2 r + \frac{4}{\pi^2}\log\frac{4}{\pi}\log r + \frac{2\theta^2}{\pi^2} + \frac{4\theta}{\pi} - \frac{2}{\pi^2}\log^2\frac{4}{\pi}\right. \\ & \left. + kr\sin\theta + O(r^2\log r)\right] + O(t^2),\end{aligned} \tag{3.20}$$

$$\eta(x,t) = t\left(\frac{2}{\pi}\log\frac{4}{\pi x} + O(x)\right) + t^2\left(\frac{2}{\pi x} + \frac{k}{2} + O(x)\right) + O(t^3) \tag{3.21}$$

as $t \to 0^+$ with $0 < r, x \ll 1$.

On comparing the terms $(-(2/\pi) r\log r\sin\theta\ldots)$ and $t(-(2/\pi^2)\log^2 r\ldots)$ in the above expansion of the potential, it is clear that these are of the same order when $r = O(-t\log r)$. This can be used iteratively to deduce that there is a non-uniformity in the expansions (3.20), (3.21) when $r = O(-t\log t)$.

3.2. *Inner region*

We now consider an inner region in which $\bar{r} = r/(-t\log t)$ and $\bar{r} = O(1)$ as $t \to 0^+$. In terms of this new coordinate, the expansions (3.20), (3.21) in the outer region, which provide matching conditions for the inner region as $\bar{r}, \bar{x} \to \infty$, take the form

$$\phi(\bar{r},\theta,t) \sim t\log^2 t\left(\frac{2}{\pi}\bar{r}\sin\theta-\frac{2}{\pi^2}\right)+t\log t\log(-\log t)\left(\frac{2}{\pi}\bar{r}\sin\theta-\frac{4}{\pi^2}\right)$$
$$+t\log t\left(\frac{2}{\pi}\bar{r}\log\bar{r}\sin\theta-\frac{2}{\pi}\left(1+\log\frac{4}{\pi}\right)\bar{r}\sin\theta+\frac{2\theta}{\pi}\bar{r}\cos\theta+\frac{4}{\pi^2}\log\frac{4}{\pi\bar{r}}\right)$$
$$-\frac{2}{\pi^2}t\log^2(-\log t)+\frac{4}{\pi^2}t\log(-\log t)\log\frac{4}{\pi\bar{r}}$$
$$+t\left(-\frac{2}{\pi^2}\log^2\bar{r}+\frac{4}{\pi^2}\log\frac{4}{\pi^2}\log\frac{4}{\pi}\log\bar{r}+\frac{2\theta^2}{\pi^2}+\frac{4\theta}{\pi}-\frac{2}{\pi^2}\log^2\frac{4}{\pi}\right)$$
$$+O(t^2\log^2 t), \quad (3.22)$$

$$\eta(\bar{x},t) \sim -\frac{2}{\pi}t\log t-\frac{2}{\pi}t\log(-\log t)+\frac{2}{\pi}t\log\frac{4}{\pi\bar{x}}+O\left(\frac{t}{\log t}\right), \quad (3.23)$$

with $\bar{x}=\bar{r}\cos\theta$ and $\bar{y}=\bar{r}\sin\theta$. In the scaled Cartesian coordinates (whose origin coincides with that of the outer coordinates (x,y)), the full problem in the inner region becomes

$$\phi_{\bar{x}\bar{x}}+\phi_{\bar{y}\bar{y}}=0 \quad \text{in} \quad \bar{x}>-\frac{1}{\log t}, \quad \frac{1}{t\log t}<\bar{y}<-\frac{\eta}{t\log t}, \quad (3.24)$$

$$\phi_{\bar{x}}=-t\log t \quad \text{on} \quad \bar{x}=-\frac{1}{\log t} \quad \text{for} \quad \frac{1}{t\log t}<\bar{y}<-\frac{\eta}{t\log t}, \quad (3.25)$$

$$-\phi_{\bar{y}}=\eta_t t\log t-\bar{x}(1+\log t)\eta_{\bar{x}}+\frac{\phi_{\bar{x}}\eta_{\bar{x}}}{t\log t} \quad \text{on} \quad \bar{y}=-\frac{\eta}{t\log t} \quad \text{for} \quad \bar{x}>-\frac{1}{\log t}, \quad (3.26)$$

$$\phi_t-\frac{\bar{x}(1+\log t)}{t\log t}\phi_{\bar{x}}-\frac{\bar{y}(1+\log t)}{t\log t}\phi_{\bar{y}}+\frac{1}{2t^2\log^2 t}\left(\phi_{\bar{x}}^2+\phi_{\bar{y}}^2\right)+\frac{\eta}{F^2}=0$$
$$\text{on} \quad \bar{y}=-\frac{\eta}{t\log t} \quad \text{for} \quad \bar{x}>-\frac{1}{\log t}. \quad (3.27)$$

It is worth noting from (3.25) that in the inner region, the plate is located at $\bar{x}=-1/\log t$, which, at leading order as $t\to 0$, is at $\bar{x}=0$. Motivated by the form of (3.22) and (3.23), we now develop expansions in the inner region of the form

$$\phi(\bar{r},\phi,t)=t\log^2 t\left(\frac{2}{\pi}\bar{r}\sin\theta-\frac{2}{\pi^2}\right)+t\log t\log(-\log t)\left(\frac{2}{\pi}\bar{r}\sin\theta-\frac{4}{\pi^2}\right)+\Phi_1 t\log t$$
$$+\Phi_2 t\log^2(-\log t)+\Phi_3 t\log(-\log t)+\Phi_4 t+\Phi_5 t^2\log^2 t$$
$$+O(t^2\log t\log(-\log t)), \quad (3.28)$$

$$\eta(\bar{x},t)=-\frac{2}{\pi}t\log t+\eta_1 t\log^2(-\log t)+\eta_2 t\log(-\log t)+\eta_3 t+\eta_4\frac{t}{\log t}+O(t^2), \quad (3.29)$$

as $t\to 0^+$ with $\bar{x},\bar{r}=O(1)$. The free surface is now located at

$$\bar{y}=\frac{2}{\pi}-\frac{\eta_1\log^2(-\log t)}{\log t}-\frac{\eta_2\log(-\log t)}{\log t}-\frac{\eta_3}{\log t}-\frac{\eta_4}{\log^2 t}+O\left(\frac{t}{\log t}\right) \quad (3.30)$$

as $t\to 0^+$ with $\bar{x}=O(1)$. Note that the above expansions must be taken to this order to deal with the switchback that occurs between the logarithmic terms. The functions $\Phi_1,\ldots\Phi_5$ are all harmonic in the quarter-plane $\bar{x}>0$, $\bar{y}<2/\pi$. The leading-order

kinematic condition is

$$\eta_1 - \bar{x}\eta_{1\bar{x}} = 0 \quad \text{on} \quad \bar{y} = \frac{2}{\pi}, \quad \bar{x} > 0. \tag{3.31}$$

The plate condition becomes $\Phi_{1\bar{x}} = -1$ at $\bar{x} = 0$, $\bar{y} < 2/\pi$ and the leading-order Bernoulli condition is

$$\Phi_1 - \bar{x}\Phi_{1\bar{x}} = 0 \quad \text{on} \quad \bar{y} = \frac{2}{\pi}, \quad \bar{x} > 0. \tag{3.32}$$

It is now convenient to shift the $\bar{y}$-coordinate, so that the leading-order free surface is located at $y' \equiv \bar{y} - 2/\pi = 0$. Using $\bar{r}^2 = \bar{x}^2 + (y' + 2/\pi)^2$ and $\theta = \tan^{-1}((y' + 2/\pi)/\bar{x})$, the matching condition for large $\bar{r}$ becomes (via (3.22))

$$\Phi_1 \sim \frac{y'}{\pi} \log\left(\bar{x}^2 + \left(y' + \frac{2}{\pi}\right)^2\right) - \frac{2y'}{\pi}\left(1 + \log\frac{4}{\pi}\right) - \frac{4}{\pi^2} + \frac{2\bar{x}}{\pi}\tan^{-1}\left(\frac{y' + \frac{2}{\pi}}{\bar{x}}\right) + o(1)$$
$$\text{as} \quad \bar{x}, -y' \to \infty. \tag{3.33}$$

This matching condition enables an immediate simplification of boundary condition (3.32). Integrating (3.32) gives $\phi_1 = A\bar{x}$ on $y' = 0$ in $\bar{x} > 0$, for some constant A. However, it follows from (3.33) on $y' = 0$ that $\phi_1 = o(1)$ as $\bar{x} \to \infty$, and hence that we must have $A = 0$. Thus the boundary condition (3.32) can be replaced by $\phi_1 = 0$ on $y' = 0$ for $\bar{x} > 0$.

We next introduce polar coordinates based on the shifted origin, so that $\bar{x} = \hat{r}\cos\hat{\theta}$, $y' = \hat{r}\sin\hat{\theta}$. In terms of these polar coordinates, the matching condition (3.33) becomes

$$\Phi_1(\hat{r}, \theta) \sim \frac{2}{\pi}\hat{r}\left\{\sin\hat{\theta}\log\hat{r} + \hat{\theta}\cos\hat{\theta} - \left[1 + \log\frac{4}{\pi}\right]\sin\hat{\theta}\right\}$$
$$+ o(1) \quad \text{as} \quad \hat{r} \to \infty, -\frac{\pi}{2} < \hat{\theta} < 0. \tag{3.34}$$

This condition is given only to $o(1)$ as $\hat{r} \to \infty$ to be consistent with the $o(1)$ truncation in the matching condition (3.33). The boundary value problem satisfied by Φ_1 is now given by

$$\nabla^2\Phi_1 = 0, \quad \hat{r} > 0, \quad -\frac{\pi}{2} < \hat{\theta} < 0,$$

together with the conditions

$$\Phi_1 = 0 \quad \text{on} \quad \hat{\theta} = 0, \quad \hat{r} > 0, \quad \frac{1}{\hat{r}}\Phi_{1\hat{\theta}} = -1 \quad \text{on} \quad \theta = -\frac{\pi}{2}, \quad \hat{r} > 0,$$

and the far-field condition, (3.34). It is readily shown that this harmonic problem has a unique solution that has ϕ_1 bounded as $\hat{r} \to 0$, and hence the solution must be

$$\Phi_1(\hat{r}, \hat{\theta}) = \frac{2}{\pi}\left(\hat{r}\sin\hat{\theta}\log\hat{r} + \hat{r}\hat{\theta}\cos\hat{\theta} - \left(1 + \log\frac{4}{\pi}\right)\hat{r}\sin\hat{\theta}\right), \quad \hat{r} \geqslant 0, \quad -\frac{\pi}{2} \leqslant \hat{\theta} \leqslant 0.$$

The free-surface elevation η_1 is given by the kinematic condition at $O(t\log t)$, which is (3.31), and this gives, on using the matching condition (3.23) as $\bar{x} \to \infty$, that $\eta_1(\bar{x}) = 0$ for $\bar{x} > 0$. By solving a similar problem to the one for Φ_1, it can be shown that $\Phi_2 = -2/\pi^2$ and $\eta_2 = -2/\pi$. At the next order, the boundary value problem that determines Φ_3 is

$$\nabla^2\Phi_3 = 0, \quad \bar{x} > 0, \quad y' < 0, \tag{3.35}$$

$$\Phi_{3y'} + \frac{2}{\pi}\Phi_{1y'y'} = 0 \quad \text{on} \quad y' = 0, \quad \bar{x} > 0, \tag{3.36}$$

$$\Phi_3 - \bar{x}\Phi_{3\bar{x}} - \frac{2}{\pi}\bar{x}\Phi_{1\bar{x}y'} + \frac{2}{\pi}\Phi_{1y'} = 0 \quad \text{on} \quad y' = 0, \quad \bar{x} > 0, \tag{3.37}$$

$$\Phi_{3\bar{x}} = 0 \quad \text{on} \quad \bar{x} = 0, \quad y' < 0, \tag{3.38}$$

$$\Phi_3 \sim \frac{4}{\pi^2} \log \frac{4}{\pi \hat{r}} \quad \text{as} \quad \hat{r} \to \infty. \tag{3.39}$$

We can use the solution for Φ_1 to establish that $\Phi_3 = (4/\pi^2)\,(\log 4/\pi - \log \hat{r})$ is the least singular solution that satisfies (3.35)–(3.39). In a similar manner, we can determine η_3, then Φ_4 and η_4. The expansions in the inner region can be summarized as

$$\begin{aligned}\phi(\hat{r}, \hat{\theta}, t) = {} & t \log^2 t \left(\frac{2}{\pi} \hat{r} \sin \hat{\theta} + \frac{2}{\pi^2} \right) + t \log t \log(-\log t) \left(\frac{2}{\pi} \hat{r} \sin \hat{\theta} \right) \\ & + t \log t \left(\frac{2}{\pi} \hat{r} \sin \hat{\theta} \log \hat{r} + \frac{2}{\pi} \hat{r} \hat{\theta} \cos \hat{\theta} - \frac{2}{\pi} \left(1 + \log + \frac{4}{\pi} \right) \hat{r} \sin \hat{\theta} \right) \\ & - \frac{2}{\pi^2} t \log^2(-\log t) + \frac{4}{\pi^2} \left(\log \frac{4}{\pi \hat{r}} \right) t \log(-\log t) \\ & + t \left(-\frac{2}{\pi^2} \left(\log \hat{r} - \log \left(\frac{4}{\pi} \right) \right)^2 + \frac{2}{\pi^2} \hat{\theta}^2 + \frac{4}{\pi} \hat{\theta} \right) + O(t^2 \log^2 t), \end{aligned} \tag{3.40}$$

$$\eta(\bar{x}, t) = -\frac{2}{\pi} t \log t - \frac{2}{\pi} t \log(-\log t) + \frac{2}{\pi} t \left(\log \frac{4}{\pi} - \log \bar{x} \right) - \frac{2}{\pi \bar{x}} \frac{t}{\log t} + O(t^2) \tag{3.41}$$

as $t \to 0^+$ with $\hat{r}, \bar{x} = O(1)$. With the solution now complete in the inner region, we can see what it tells us about the physical problem. The leading-order term has changed from the pressure impulse to a purely vertical flow with speed of $O(-\log t)$ and we are starting to see the fast vertical motion of the root of the nascent jet.

We now observe, via (3.41), that the free-surface elevation is still unbounded as $\bar{x} \to 0$. This suggests that a further region will be required to produce a bounded solution.

3.3. *Inner-inner region*

A careful inspection of the structure of the equations of motion in the previous regions reveals that we neglected a term in the kinematic condition of $O(t \log t \Phi_{1\bar{y}}) = O(t \log t \log \hat{r})$ and retained a term of $O(t \log t \log(-\log t))$. When $\hat{r} \to 0$ these balance when $\hat{r} = O(1/\log t)$ and so we introduce an inner-inner region in terms of the new variables $\tilde{r} = (-\hat{r} \log t)$, $\tilde{\theta} = \hat{\theta}$. This gives the matching conditions from the inner region for $\tilde{r}, \tilde{x} \gg 1$ as

$$\begin{aligned}\phi(\tilde{r}, \tilde{\theta}, t) \sim {} & \frac{2}{\pi^2} t \log^2 t - \frac{2}{\pi} \tilde{y} t \log t + t \left(-\frac{2}{\pi} \tilde{r} \sin \tilde{\theta} \log \tilde{r} - \frac{2}{\pi} \tilde{r} \tilde{\theta} \cos \tilde{\theta} \right. \\ & \left. + \frac{2}{\pi} \tilde{r} \sin \tilde{\theta} \left(1 + \log \frac{4}{\pi} \right) - \frac{2}{\pi^2} \left(\log \tilde{r} - \log \frac{4}{\pi} \right)^2 + \frac{2}{\pi^2} \tilde{\theta}^2 + \frac{4}{\pi} \tilde{\theta} \right) + O(t^2 \log^2 t), \end{aligned} \tag{3.42}$$

$$\eta(\tilde{x}, t) \sim -\frac{2}{\pi} t \log t + \frac{2}{\pi} t \left(\log \frac{4}{\pi} - \log \tilde{x} + \frac{1}{\tilde{x}} \right) + O\left(\frac{t}{\log t} \right) \tag{3.43}$$

as $t \to 0^+$. Here $\tilde{x} = \tilde{r} \cos \tilde{\theta}$, $\tilde{y} = \tilde{r} \sin \tilde{\theta}$. In the inner-inner region the full equations and boundary conditions are

$$\nabla^2 \phi = 0 \quad \text{in} \quad \tilde{x} > 1, \quad \frac{2}{\pi} \log t - \frac{1}{t} < \tilde{y} < \frac{\eta}{t} + \frac{2}{\pi} \log t, \tag{3.44}$$

$$\phi_{\tilde{x}} = t \quad \text{on} \quad \tilde{x} = 1, \quad \frac{2}{\pi} \log t - \frac{1}{t} < \tilde{y} < \frac{\eta}{t} + \frac{2}{\pi} \log t, \tag{3.45}$$

$$\phi_{\tilde{y}} = t\eta_t - \tilde{x}\eta_{\tilde{x}} + \frac{1}{t}\phi_{\tilde{x}}\eta_{\tilde{x}} \quad \text{on} \quad \tilde{y} = \frac{\eta}{t} + \frac{2}{\pi}\log t, \quad \tilde{x} > 1, \tag{3.46}$$

$$\phi_t = \frac{\tilde{x}}{t}\phi_{\tilde{x}} + \frac{\tilde{y}}{t}\phi_{\tilde{y}} - \frac{2}{\pi t}(1+\log t)\phi_{\tilde{y}} - \frac{1}{2t^2}\left(\phi_{\tilde{x}}^2 + \phi_{\tilde{y}}^2\right) - \frac{\eta}{F^2} \quad \text{at} \quad \tilde{y} = \frac{\eta}{t} + \frac{2}{\pi}\log t, \quad \tilde{x} > 1. \tag{3.47}$$

The matching conditions (3.42) and (3.43) lead us to the following expansions in the inner-inner region:

$$\phi(\tilde{x}, \tilde{y}, t) = \frac{2}{\pi^2} t \log^2 t - \frac{2}{\pi}\tilde{y} t \log t + \Phi_1 t + O(t^2 \log^2 t), \tag{3.48}$$

$$\eta(\tilde{x}, t) = -\frac{2}{\pi} t \log t + \eta_1 t + O(t/\log t) \tag{3.49}$$

as $t \to 0^+$. On substitution from (3.48), (3.49) into (3.42)–(3.47) we obtain the leading-order problem, which determines Φ_1 and η_1, as

$$\nabla^2 \Phi_1 = 0 \quad \text{in} \quad \tilde{x} > 1, \quad -\infty < \tilde{y} < \eta_1, \tag{3.50}$$

$$\Phi_{1\tilde{x}} = 1 \quad \text{on} \quad \tilde{x} = 1, \quad -\infty < \tilde{y} < \eta_1, \tag{3.51}$$

$$-\frac{2}{\pi}\eta_1 + \Phi_1 - \tilde{x}\Phi_{1\tilde{x}} - \eta_1 \Phi_{1\tilde{y}} + \frac{2}{\pi}\Phi_{1\tilde{y}} + \frac{1}{2}\left(\Phi_{1\tilde{x}}^2 + \Phi_{1\tilde{y}}^2\right) = 0 \quad \text{on} \quad \tilde{y} = \eta_1, \quad \tilde{x} > 1 \tag{3.52}$$

$$\Phi_{1,\tilde{y}} = -\frac{2}{\pi} + \eta_1 - \tilde{x}\eta_{1\tilde{x}} + \Phi_{1\tilde{x}}\eta_{1\tilde{x}} \quad \text{on} \quad \tilde{y} = \eta_1, \quad \tilde{x} > 1, \tag{3.53}$$

$$\Phi_1 \sim \Phi_\infty = -\frac{2}{\pi}\tilde{r}\sin\tilde{\theta}\log\tilde{r} + \frac{2\tilde{r}}{\pi}\sin\tilde{\theta}\left(1 + \log\frac{4}{\pi}\right) - \frac{2}{\pi}\tilde{r}\tilde{\theta}\cos\tilde{\theta} - \frac{2}{\pi^2}\left(\log\tilde{r} - \log\frac{4}{\pi}\right)^2 + \frac{2}{\pi^2}\tilde{\theta}^2 + \frac{4}{\pi}\tilde{\theta} \quad \text{as} \quad \tilde{r} \to \infty, \quad -\frac{\pi}{2} < \tilde{\theta} < 0, \tag{3.54}$$

$$\eta_1 \sim \eta_\infty = \frac{2}{\pi}\left(-\log\tilde{x} + \log\frac{4}{\pi} + \frac{1}{\tilde{x}}\right) \quad \text{as} \quad \tilde{x} \to \infty. \tag{3.55}$$

This problem is a fully nonlinear free boundary problem, so its solution must be determined by numerical methods. Since it contains no parameters, it only has to be computed once. Of course if the solution is singular at the point where the free surface meets the plate, we would require further asymptotic regions. However a local analysis of the flow and free surface reveal this not to be the case. In fact, (3.50)–(3.55) has a local solution in which $\eta_1(\tilde{x})$ has a finite limit as $\tilde{x} \to 1$, and which touches the plate at $\tilde{x} = 1$ tangentially, namely†

$$\eta_1(\tilde{x}) \sim k_0 - k_1(\tilde{x} - 1)^{2/3} \quad \text{as } \tilde{x} \to 1, \tag{3.56}$$

where k_0 and k_1 are positive constants that cannot be determined locally. Moreover, $\Phi_1(\tilde{x}, \tilde{y})$ is regular at this contact point, and so $\nabla\Phi_1(\tilde{x}, \tilde{y})$ is bounded there. In particular, we find that

$$\Phi_1(\tilde{x}, \tilde{y}) \sim \frac{1}{2}\left(k_0^2 + \frac{4}{\pi^2} + 1\right) - \left(k_0 - \frac{2}{\pi}\right)(k_0 - \tilde{y}) + (\tilde{x} - 1) \quad \text{as } (\tilde{x}, \tilde{y}) \to (1, k_0). \tag{3.57}$$

† Note that there is also a local solution with the free surface perpendicular to the wall at the contact point, but our numerical investigation of the problem indicates that this is not the local structure appropriate to the solution of the full problem.

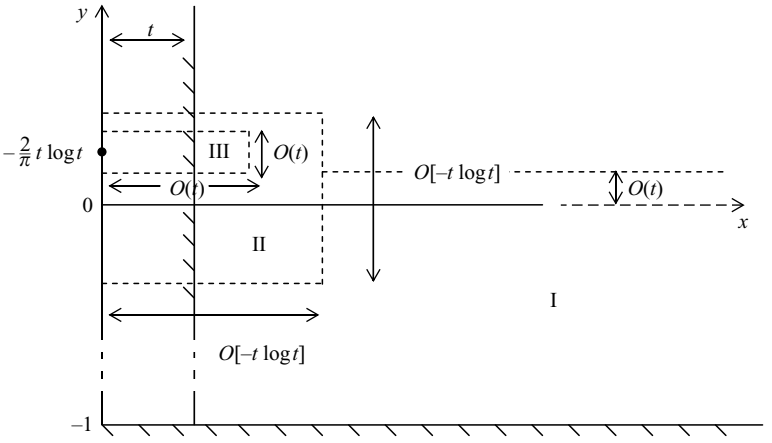

FIGURE 3. Asymptotic structure as $t \to 0^+$. I is the outer region, II is the inner region, III is the inner-inner region.

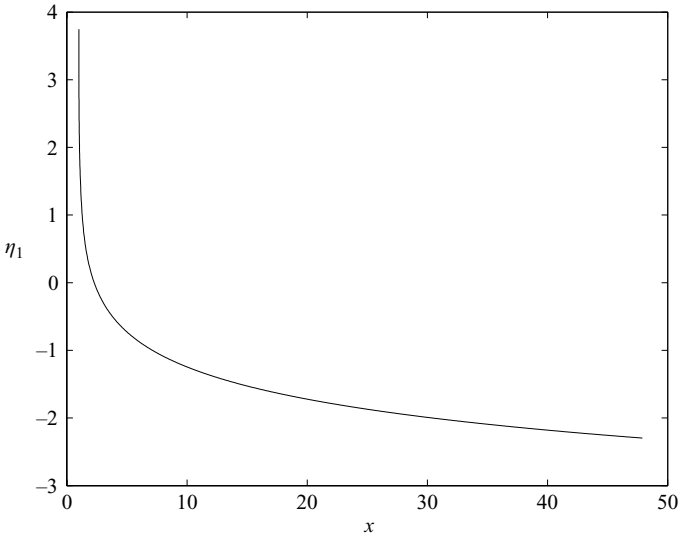

FIGURE 4. The numerically calculated solution in the inner-inner region. Note that the value $\eta_1(0) \approx 4.3$ is obtained by extrapolation from unconverged numerical solutions. The solution shown has an arclength of 50 and is calculated using 1080 boundary elements.

The asymptotic structure as $t \to 0^+$ is now complete, and is illustrated in figure 3. The solution of the nonlinear free boundary problem (3.50)–(3.55) is shown in figures 4 and 5. The numerical techniques that we used to obtain it are discussed in the Appendix. Specifically, the numerical solution determines that $k_0 \approx 4.3$ and $k_1 \approx 4 \times 10^{-3}$.

4. Conclusions

The impulsive flow caused by a vertical plate moving into a stationary strip of inviscid incompressible fluid has been studied in the small time limit. The structure of the flow field is revealed using the method of matched asymptotic expansions. It is found that three asymptotic regions are necessary to describe the flow. After

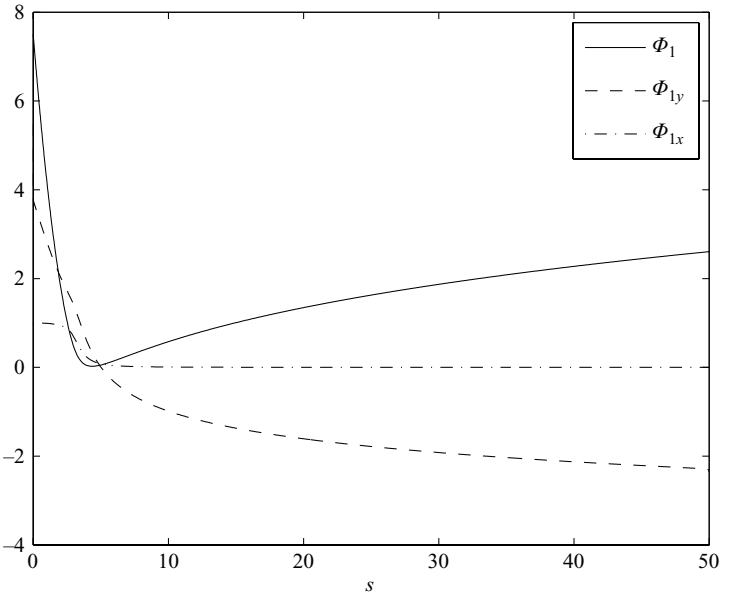

FIGURE 5. The potential on the free surface and its derivatives for the numerically calculated solution in the inner-inner region.

analysing an $O(1)$ outer region, in which the free-surface elevation and velocities are unbounded at the point where the free surface meets the plate, an inner region of size $O(-t\log t)$ centred at the point where the free surface initially meets the plate must be introduced. Since there are still singularities, albeit weaker than in the $O(1)$ region, this is augmented by an inner-inner region of size $O(t)$, centred on a nascent jet rising vertically up the plate in response to the impulsive horizontal motion. The equations that govern the motion in this region are nonlinear and parameter free, and a numerical solution is shown in figures 4 and 5.

In the neighbourhood of the point where the free surface meets the plate, when $\tilde{x}=1+o(1)$ and $\tilde{y}=k_0+o(1)$ (that is $x=t+o(t)$ and $y=-(2/\pi)t\log t+k_0t+o(t)$) as $t\to 0^+$, we have, from (3.48) and (3.49) together with (3.56) and (3.57), that,

$$\eta(\tilde{x},t)=-\frac{2}{\pi}t\log t+\left\{k_0-k_1(\tilde{x}-1)^{2/3}+o\left((\tilde{x}-1)^{2/3}\right)\right\}t+O\left(\frac{t}{\log t}\right), \tag{4.1}$$

and

$$\phi_x(\tilde{x},\tilde{y},t)=\left\{1+O\left((\tilde{x}-1),(\tilde{y}-k_0)\right)\right\}+O(t\log^2 t), \tag{4.2}$$

$$\phi_y(\tilde{x},\tilde{y},t)=-\frac{2}{\pi}\log t+\left\{\left(k_0-\frac{2}{\pi}\right)+O\left((\tilde{x}-1),(\tilde{y}-k_0)\right)\right\}+O(t\log^2 t) \tag{4.3}$$

as $t\to 0^+$, with $(\tilde{x}-1,\tilde{y}-k_0)=o(1)$ and $k_0\approx 4.3$, $k_1\approx 4\times 10^{-3}$, these constants being determined numerically (see the Appendix). It should be noted from (4.1) that the free surface leaves the plate tangentially at $\tilde{x}=1$, and from (4.2) and (4.3) that the fluid velocity is finite at this tangency point between the free surface and the plate, when $t>0$, as required, becoming singular only as $t\to 0^+$.

In physical terms, the structure in the inner-inner region, where $x=O(t)$ and $y=-(2/\pi)t\log t+O(t)$, is that of a predominantly vertical jet with flow speed $-(2/\pi)\log t+O(1)$ and thickness $O(t)$ with height $-(2/\pi)t\log t+k_0t+o(1)$. This

jet is accommodated into the more passive flow in the outer region, where the flow speed is $O(1)$ as $t \to 0$, via a transition within the thicker inner region, where $(x, y) = O(-t \log t)$. It should be noted that any numerical scheme developed to solve the full initial-boundary value problem (2.2)–(2.7) must be able to adapt to the $O(t)$ and $O(t \log t)$ length scales in the inner-inner and inner regions as $t \to 0^+$, if it is to resolve accurately the structure of the flow near the point where the free surface meets the plate.

It is worth concluding by contrasting our results with those for the case of a plate moving into the stationary strip of fluid with constant acceleration, as studied in detail by King & Needham (1994). In this situation, no inner-inner region is required, and a predominantly vertical jet develops in the inner region, where $(x, y) = O(-t^2 \log t)$. The flow speed in the jet is $-(8\sigma/\pi)t \log t + O(t)$ and the jet thickness is $O(-t^2 \log t)$ with height $-(4\sigma/\pi)t^2 \log t + O(t^2)$. Here, σ is the dimensionless initial acceleration of the plate. Thus whilst the momentum flux in the jet formed by a plate moving at constant speed is $O(t \log^2 t)$, that formed by a plate moving with constant acceleration has momentum flux $O(t^4 \log^3 t)$ as $t \to 0^+$. The jet formed is therefore significantly more violent for the impulsively started plate than for the smoothly accelerated plate, as we would expect. We also note that for the smoothly accelerated plate, the free surface meets the plate at a finite angle, rather than tangentially, with slope of $O(1/\log t)$ (King & Needham 1994).

Finally, we note that, to the order we have developed the expansions in each of the outer, inner and inner-inner regions, the effect of gravity, through the Froude number F, does not appear. At early times, gravity therefore plays no significant role in the formation of the jet.

Appendix. Numerical solution of the inner-inner problem

The inner-inner problem given by (3.50)–(3.55) is a nonlinear free boundary problem, and contains no parameters. Since the field equation is Laplace's equation, it makes sense to reduce this two-dimensional boundary value problem to a one-dimensional set of ordinary differential equations coupled to an integral equation by using the boundary integral method. We begin by reformulating the problem into a more convenient form.

A.1. *Reformulation*

Our first step is to define the position of the free surface parametrically in terms of arclength, s, as $\eta_1 = \tilde{Y}(s)$, $\tilde{x} = \tilde{X}(s)$, with $s = 0$ at the point where the free surface meets the plate and s increasing along the free surface. In order to simplify our notation, we also define $\tilde{\phi} \equiv \Phi_1(\tilde{x}, \tilde{y})$ and the potential on the free surface, $\tilde{\Phi} \equiv \tilde{\phi}(\tilde{X}(s), \tilde{Y}(s))$. Our second step is to shift the $\tilde{y}$-axis to the wall and subtract the velocity of the wall by defining $x \equiv \tilde{x} - 1$, $y \equiv \tilde{y}$, $X \equiv \tilde{X} - 1$, $Y \equiv \tilde{Y}$, $\phi \equiv \tilde{\phi} - x$, $\Phi \equiv \tilde{\Phi} - X$. Note that these variables are not to be confused with the original variables used in the outer region.

We now have a boundary value problem for Laplace's equation with $\partial\phi/\partial x = 0$ at $x = 0$. The problem in $x > 0$, $y < Y$ is therefore equivalent to a problem in $-\infty < x < \infty$, $y < Y$ with symmetry about the y-axis. In terms of these new variables, we must solve

$$\nabla^2 \phi = 0 \quad \text{in } -\infty < x < \infty,\ y < Y, \tag{A 1}$$

subject to

$$\frac{1}{2}\Phi'^2 - \left(XX' + YY' - \frac{2}{\pi}Y'\right)\Phi' + \Phi - \frac{2}{\pi}Y - \frac{1}{2} - \frac{1}{2}\left(X'Y - Y'X - \frac{2}{\pi}X'\right)^2 = 0$$
$$\text{on } x = X(s),\ y = Y(s), \tag{A 2}$$

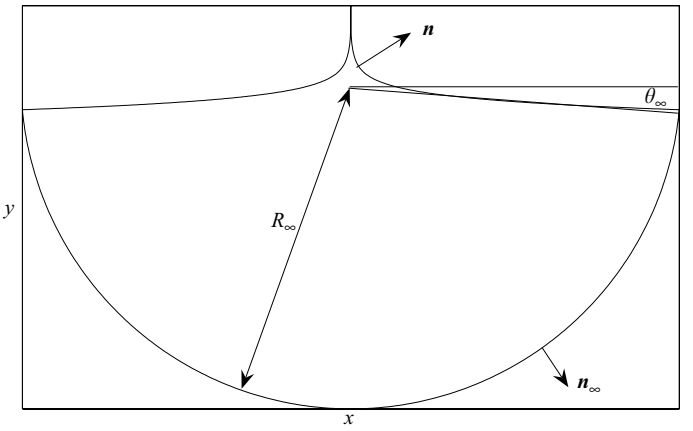

FIGURE 6. The domain of solution for the reformulated inner-inner problem.

$$\boldsymbol{n}\cdot\nabla\phi = YX' - XY' - \frac{2}{\pi}X' \quad \text{on } x = X(s),\ y = Y(s), \tag{A 3}$$

where a prime denotes $\mathrm{d}/\mathrm{d}s$ and $\boldsymbol{n}$ is the outward unit normal. The far-field conditions are

$$\phi \sim \phi_\infty \equiv -\frac{2y}{\pi}\left\{\log\left(\frac{\pi r}{4}\right) - 1\right\} - x\left(1 + \frac{2\theta}{\pi}\right) - \frac{2}{\pi^2}\left\{\log\left(\frac{\pi r}{4}\right)\right\}^2 + \frac{2\theta}{\pi}\left(1 + \frac{\theta}{\pi}\right) + o(1) \quad \text{as } r \to \infty,\ -\pi < \theta < 0 \tag{A 4}$$

$$Y = -\frac{2}{\pi}\log\left(\frac{\pi|X|}{4}\right) + o\left(\frac{1}{X}\right) \quad \text{as } |X| \to \infty, \tag{A 5}$$

where (r, θ) are polar coordinates centred at the origin. We also have symmetry about the y-axis. Finally, the arclength condition is

$$X'^2 + Y'^2 = 1. \tag{A 6}$$

Since we know that the local solution on the free surface close to the y-axis takes the form given by (3.56), we find that we must solve Laplace's equation in a semi-infinite domain with a cusp at $x = 0$, $y = Y(0)$.

A.2. *Numerical method*

In order to use the boundary integral method, we truncate the domain of solution with an arc of the circle centred at the origin that passes through $(X(s_\infty), Y(s_\infty))$ and, by symmetry, $(X(-s_\infty), Y(-s_\infty)) = (-X(s_\infty), Y(s_\infty))$, for some suitably large positive constant s_∞. We denote the radius of this circle by R_∞, and the angle that a line from the origin to the point $(X(s_\infty), Y(s_\infty))$ makes with the x-axis by θ_∞, as illustrated in figure 6. On this truncated domain, we can replace Laplace's equation by the boundary integral representation

$$\Phi(s_0) = -\frac{1}{\pi}\int_{-s_\infty}^{s_\infty}\left\{\log\rho(s, s_0)\boldsymbol{n}\cdot\nabla\phi(s) + \frac{\boldsymbol{n}\cdot(\boldsymbol{x}_0 - \boldsymbol{x})}{\rho^2(s, s_0)}\Phi(s)\right\}\mathrm{d}s + I_\infty, \tag{A 7}$$

where

$$I_\infty \equiv -\frac{R_\infty}{\pi}\int_{-\theta_\infty}^{-\pi+\theta_\infty}\left\{\log R(\theta, s_0)\frac{\partial\phi_\infty}{\partial r}(R_\infty, \theta) + \frac{\boldsymbol{n}_\infty(\theta)\cdot(\boldsymbol{x}_0 - \boldsymbol{x}_\infty)}{R^2(\theta, s_0)}\phi_\infty(R_\infty, \theta)\right\}\mathrm{d}\theta, \tag{A 8}$$

and

$$\boldsymbol{x} \equiv (X(s), Y(s)), \quad \boldsymbol{x}_0 \equiv (X(s_0), Y(s_0)), \quad \boldsymbol{x}_\infty \equiv (R_\infty \cos\theta, R_\infty \sin\theta),$$
$$\rho(s, s_0) \equiv |\boldsymbol{x} - \boldsymbol{x}_0|, \quad R(\theta, s_0) \equiv |\boldsymbol{x}_\infty - \boldsymbol{x}_0|, \quad \boldsymbol{n}_\infty \equiv (\cos\theta, \sin\theta), \quad \boldsymbol{n} \equiv (-Y', X').$$

Note that I_∞, the contribution from the arc at infinity, does not vanish as $R_\infty \to \infty$, and must be approximated numerically, as discussed below.

We must now solve (A 7), with $\boldsymbol{n}\cdot\nabla\phi$ given by (A 3), along with the ordinary differential equations (A 2) and (A 6), subject to the far-field conditions (A 4) and (A 5), symmetry and $X(0) = 0$. We represent the free surface in $x > 0$ with $N-1$ straight line segments, which meet at the N nodes $(X_i, Y_i) \equiv (X(s_i), Y(s_i))$ for $i = 1, 2, \ldots, N$ with $s_1 = 0$ and $s_N = s_\infty$. We represent the potential at the free surface, Φ, with $\Phi = \Phi_i$ at $s = s_i$, and assume that Φ varies linearly between the nodes. This gives us $3N$ unknowns. For these linear elements, the integral in (A 7) can be evaluated analytically, taking the symmetry of the problem into account. Collocating at the $N-1$ midpoints of the elements, $s_0 = \frac{1}{2}(s_i + s_{i-1})$ for $i = 1, 2, \ldots, N-1$, this leads to $N-1$ nonlinear algebraic equations.

Evaluating the integral on each element analytically has two advantages over approximate evaluation of the integral, for example using Gaussian quadrature. Firstly, the weak, logarithmic singularity in the integral is dealt with explicitly. Moreover, when the collocation point is close to the y-axis, which it will be for a large number of elements because of the cusp in the free surface, there will also be an almost singular integral associated with the image of the collocation point in the y-axis. This is dealt with exactly by the analytical evaluation of the integral. Secondly, when we come to solve our final system of nonlinear algebraic equations using Newton's method, we can calculate the Jacobian of the system analytically. If we were to use an approximate method to evaluate the integral, we would need to obtain the Jacobian by finite differences. This takes far longer, certainly an order of magnitude longer, than the time spent on inverting the Jacobian, and would then be the main, severely restrictive, bottleneck in the numerical calculation.

We evaluate the integral I_∞ by subdividing the range of integration and using two, point Gaussian quadrature on each of these subintervals. At the end of the arc close to the point $(X(s_\infty), Y(s_\infty))$, we subdivide an interval of arclength $10\,\mathrm{d}s_\infty$ into 100 subintervals, where $\mathrm{d}s_\infty \equiv s_N - s_{N-1}$ is the node spacing at the end of the free surface. This is essential, in order to resolve the rapid variation of the far field when the collocation point is nearby. The remainder of the range of integration is divided into subintervals of length approximately $\sqrt{\mathrm{d}s_\infty}$, exploiting the high accuracy of Gaussian quadrature to evaluate the integral efficiently. Note that, when we use Newton's method, we evaluate the part of the Jacobian that arises from I_∞ using finite differences, since it is not tractable to do this analytically. This can be done efficiently as it only depends upon X_N and Y_N.

We solve (A 2) at the $N-2$ interior nodes, evaluating the first derivatives using a four-point finite difference approximation. It has been found previously that the more obvious three-point approximation leads to a numerical instability (Billingham & King 2005). We solve (A 6) on each of the $N-1$ linear elements, which basically ensures that the length of each element is as specified by the difference of the prescribed values of $s = s_i$ at the end points of each node. This gives us $3N-4$ nonlinear algebraic equations for the $3N$ unknowns. The remaining four equations are given by the conditions (A 4) and (A 5) on the far-field potential and free-surface position respectively, along with $X(s_1) = X'(s_1) = 0$.

To solve these nonlinear algebraic equations, we use Newton's method. However, in order to proceed, we need an initial guess of the solution. There are no parameters in these equations, and no obvious initial guess with which to start our calculation. In order to reach the solution, we introduce three artificial continuation parameters, σ, ϵ and α, and modify (A 3), (A 4), (A 5) and one of the boundary conditions at the plate, so that

$$\boldsymbol{n}\cdot\nabla\phi = YX' - XY' - \frac{2}{\pi}X' + \sigma(X'Y'' - Y'X''), \quad \text{on } x = X(s),\ y = Y(s), \tag{A 9}$$

$$\begin{aligned}\phi(s_\infty) = (1-\epsilon)\left[-\frac{2Y(s_\infty)}{\pi} + \frac{2}{\pi^2} + \frac{1}{2}\right] + \epsilon\left[-\frac{2Y}{\pi}\left\{\log\left(\frac{\pi R_\infty}{4}\right) - 1\right\}\right.\\ \left. - X\left(1 - \frac{2\theta_\infty}{\pi}\right) - \frac{2}{\pi^2}\left\{\log\left(\frac{\pi R_\infty}{4}\right)\right\}^2 - \frac{2\theta_\infty}{\pi}\left(1 - \frac{\theta_\infty}{\pi}\right)\right],\end{aligned} \tag{A 10}$$

$$Y(s_\infty) = -\frac{2\epsilon}{\pi}\log\left(\frac{\pi X}{4}\right), \tag{A 11}$$

$$Y'(s_1)\cos\alpha = X'(s_1)\sin\alpha. \tag{A 12}$$

Now, when $\alpha = 0$ and $\epsilon = 0$, there is a simple solution for any σ, namely

$$Y = 0, \quad X = s, \quad \phi = -\frac{2y}{\pi} + \frac{2}{\pi^2} + \frac{1}{2}.$$

This is the starting point for our continuation method. The inclusion of the extra term in (A 9) is inspired by the diffusive term introduced into the kinematic boundary condition by Cokelet & Longuet-Higgins (1976) to stabilize their method of solving the unsteady water wave equations. By introducing this term into our kinematic condition, we are able to impose a contact angle condition through (A 12). When $\epsilon = 1$, $\sigma = 0$ and $\alpha = -\pi/2$, we recover the boundary value problem that we are interested in. We proceed in three stages. First, with $\sigma > 0$, typically $\sigma = 0.1$, and $\alpha = 0$, we increase ϵ from 0 to 1 in small steps, using the solution from the preceding value of ϵ as the initial guess for the new solution. We then decrease α from 0 to $-\pi/2$, in steps that decrease as $-\pi/2$ is approached. Finally, we gradually decrease σ to zero, until we have a solution of the boundary value problem we are interested in. We space the nodes in a non-uniform manner, with the node spacings, $\Delta s_i \equiv s_{i+1} - s_i$, varying from a small value close to $s = 0$ up to a larger value as s approaches s_∞.

Unfortunately, we find that there is a weak numerical instability using this method, which manifests itself as a grid-scale oscillation in the four or five nodes closest to $s = 0$, the point where the free surface meets the wall. However, we find that by taking σ small, we can obtain a smooth, converged solution, and extrapolate to find the position of the tip when $\sigma = 0$.

A.3. *Results*

In the following results, the node spacing is 10^{-2} close to $s = 0$, and increases to 0.1 as s approaches $s_\infty = 25$, with $N = 317$. Figure 7 shows how the free surface close to the contact point changes as α decreases. We can see that the solution approaches the expected cusp, with the solution away from the immediate neighbourhood of the contact point unaffected. In order to estimate $Y(0)$, the position of the contact point, we fit a curve of the form $y = Y(0) - k_1 x^{2/3}$ to the solution close to the contact point. A typical example is shown in figure 7.

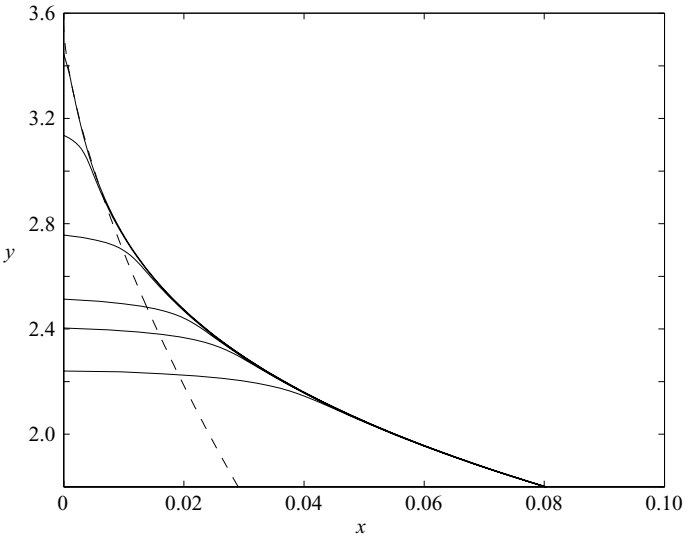

FIGURE 7. The calculated free surface as α varies, with $\sigma = 0.01$ and $\alpha = 0, -\pi/6, -\pi/4, -3\pi/8, -\pi/2 + 0.1$ and $-\pi/2$. The broken line is the curve fitted to the solution with $\alpha = -\pi/2$, from which we deduce $Y(0)$. Note the large difference in scales between the x and y axes.

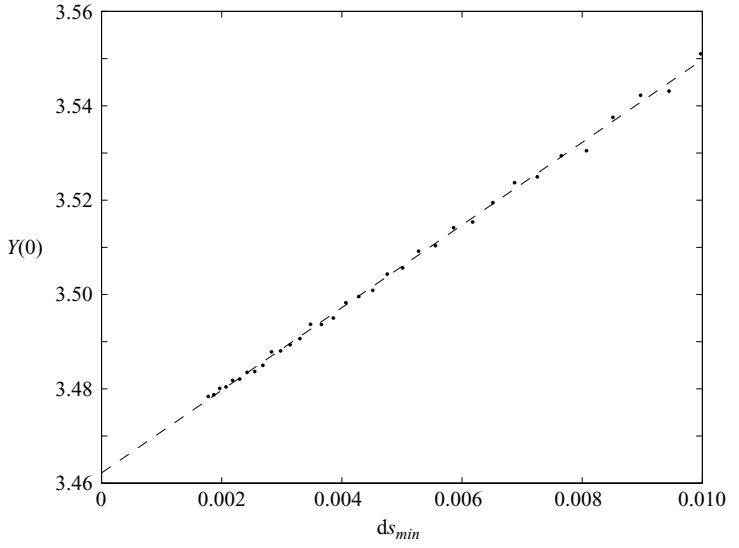

FIGURE 8. The calculated value of $Y(0)$ as $\mathrm{d}s_{min}$ varies, with $s_\infty = 25$, along with the best fit straight line.

In order to investigate the convergence of the numerical solution as we reduce the node spacing, we begin with the solution for $\sigma = 10^{-2}$ and successively, uniformly shrink the nodal distribution, adding extra nodes to keep $s_\infty = 25$, and also reduce σ, taking $\sigma = s_2 - s_1$. We do this since we expect, and indeed find, that the size of the region close to the contact point, where the solution is not of the correct form, scales with σ, and we can make this smaller as the grid spacing decreases. Figure 8 shows how the calculated value of $Y(0)$ varies with the smallest nodal spacing, $\mathrm{d}s_{min} \equiv s_2 - s_1$. As we would expect for linear boundary elements, $Y(0)$ varies linearly with $\mathrm{d}s_{min}$.

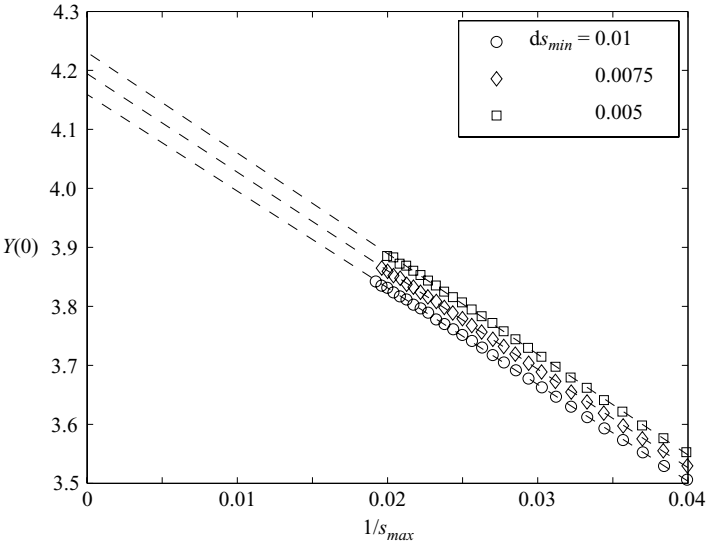

FIGURE 9. The calculated value of $Y(0)$ as s_∞ varies, along with the best-fit straight lines for $\mathrm{d}s_{min} = 0.01$, 0.0075 and 0.005.

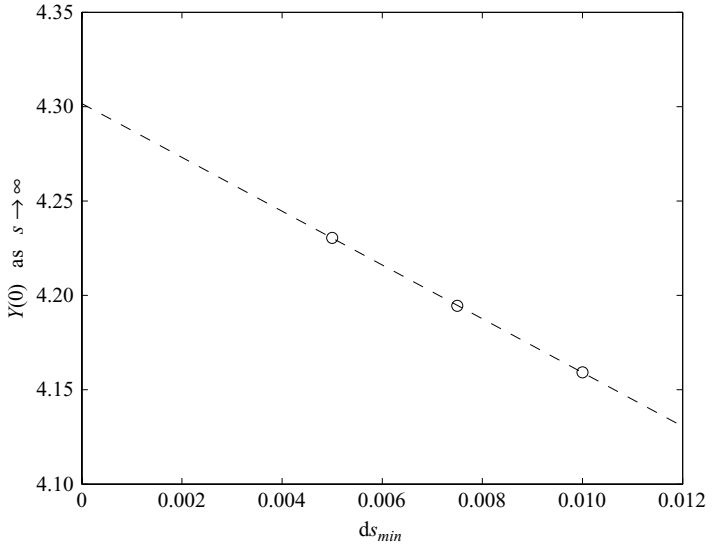

FIGURE 10. The calculated value of $Y(0)$ as $s_\infty \to \infty$ for $\mathrm{d}s_{min} = 0.1$, 0.075 and 0.05, along with the best-fit straight line.

Finally, to test the convergence of the solution as s_∞ grows, we again start from the solution with $\sigma = 10^{-2}$ and successively increase s_∞, keeping the spacing of the new nodes constant at 0.1. We find that the position of the tip varies approximately linearly with $1/s_\infty$, as shown in figure 9, as we would expect, since this is the order of the error incurred by evaluating I_∞ at finite s_∞. The best-fit straight line can be extrapolated to find our best estimate of $Y(0)$ as $s_\infty \to \infty$. We repeat this with initial node spacings scaled by 0.75 and 0.5, also shown in figure 9. This gives us the estimates of $Y(0)$ shown in figure 10, which we then extrapolate (cf. figure 8) to give

our final estimate, $Y(0) \approx 4.3$. The solution shown in figure 4 and 5 has $s_\infty = 50$ and $\mathrm{d}s_{min} = 0.005$.

REFERENCES

Batchelor, G. K. 1967 *Introduction to Fluid Dynamics*. Cambridge University Press.

Billingham, J. & King, A. C. 2005 Surface tension-driven flow outside a slender wedge with an application to the inviscid coalescence of drops. *J. Fluid Mech.* **533**, 193–221.

Cointe, R. & Armand, J.-L. 1987 Hydrodynamic impact analysis of a cylinder. *ASME J. Offshore Mech. Arc. Engng* **109**, 237.

Cointe, R. 1989 Solid-liquid impact analysis. *ASME J. Offshore Mech. Arc. Engng* **111**, 109.

Greenhow, M. & Lin, W. M. 1983 Nonlinear free surface effects: experiment and theory. *Rep* 83-19. Dept Ocean Engng, MIT.

Howison, D., Ockendon, J. & Wilson S. K. 1991 Wedge entry problems at small deadrise angle. *J. Fluid Mech.* **222**, 215–230.

King, A. C. & Needham, D. J. 1994 The initial development of a jet caused by fluid, body and free-surface interaction. Part 1. A uniformly accelerating plate. *J. Fluid Mech.* **268**, 89–101.

Longuet-Higgins, M. S. & Cokelet, E. D. 1976 The deformation of steep surface waves on water I. A numerical method of computation. *Proc. R. Soc. Lond.* A **350**, 1–33.

Yong, S. A. & Chwang, A. T. 1992 Experimental study of waves produced by an accelerating plate. *Phys. Fluids* A **4**, 2456.